miR-27b-3p and miR-607 cooperatively regulate BLM gene expression by directly targeting the 3'-UTR in PC3 cells

YINGLIAN CHEN[1-4], JIAFU ZHAO[1,2], ZHIQIANG DUAN[1,2], TING GONG[1,2], WEI CHEN[1,2], SAINAN WANG[1-3] and HOUQIANG XU[1-4]

[1]Key Laboratory of Animal Genetics, Breeding and Reproduction in The Plateau Mountainous Region, Ministry of Education; [2]Key Laboratory of Animal Genetics, Breeding and Reproduction; [3]College of Life Science; [4]Medical College, Guizhou University, Guiyang, Guizhou 550025, P.R. China

Received July 11, 2018; Accepted March 26, 2019

DOI: 10.3892/mmr.2019.10135

Abstract. BLM RecQ like helicase (BLM) has a pivotal role in genetic recombination, transcription, DNA replication and DNA repair, which presents the possibility of using BLM as an anti-cancer target for treatment. However, the post-transcriptional control regulation of BLM gene expression is not fully understood and limits the application of drugs targeting BLM for carcinoma therapy in the future. MicroRNAs (miRNAs) inhibit gene expression through interaction with the 3' untranslated region (3'-UTR) of mRNA at the post-transcriptional stage. Therefore, the current study screened for miRNAs that regulate BLM gene expression, with software predicting that miRNA (miR)-27b-3p, miR-607, miR-361-3p, miR-628-5p and miR-338-3p. BLM gene expression levels in the PC3 prostate cancer cell line and RWPE-2 normal prostate epithelium cell line were detected by reverse transcription-quantitative PCR. Additionally, BLM mRNA levels were following miRNA overexpression for 24 and 48 h. For further miRNA filtration and validation, a dual-luciferase reporter system and western blot analysis were performed, which demonstrated that miR-27b-3p and miR-607 reduce BLM gene expression by directly targeting the BLM mRNA 3'-UTR. A Box-Behnken design experiment suggested that miR-27b-3p and miR-607 have synergetic mutual effects on BLM gene expression. Finally, the suppressive effect of miR-27b-3p and miR-607 on PC3 cell proliferation, colony formation, migration and invasion indicated the benefit of studying BLM as a drug target in cancer. In conclusion, the findings of the current provide evidence that miR-27b-3p and miR-607 have an oncosuppressive function in PC3 cells and cooperatively downregulate BLM expression at the post-transcriptional level.

Correspondence to: Professor Houqiang Xu, Key Laboratory of Animal Genetics, Breeding and Reproduction in The Plateau Mountainous Region, Ministry of Education, Guizhou University, 2,708, South Section, Huaxi Avenue, Guiyang, Guizhou 550025, P.R. China
E-mail: gzdxxhq@163.com

Key words: BLM RecQ like helicase, microRNA, prostate cancer, Pfaffl arithmetic, Box-Behnken design

Introduction

Prostate cancer is the second leading cause of cancer-associated mortality in males worldwide (1). Nowadays, conventional drugs such as cis-platinum and mitomycin are usually selected for use as auxiliaries in chemotherapy or radiotherapy for prostate carcinoma treatment (2,3). Several studies have directly or indirectly implied that patients with terminal cancer could be treated in the future using drugs targeting critical endogenous factors such as Her2/Neu, epidermal growth factor or tumor necrosis factor-α (2-5). Improved target selection of anti-cancer drugs is very important for clinical research. BLM RecQ like helicase (BLM) is a member of the RecQ helicase family that has a pivotal role in genetic recombination, transcription, DNA replication and DNA repair. BLM gene defects can cause Bloom syndrome, accompanied by cancer predisposition (6-9). A recent study indicated that knockdown of BLM impairs the normal proliferation and metabolism of cancer cells (5). Drugs targeting BLM have been used to treat cancer (5,10-14). However, the majority of anti-cancer drugs are ineffective due to poor target specificity, and certain regulation mechanisms, such as the post-transcriptional control pathway of BLM gene expression, remain unclear, which limits the application of drugs targeting BLM for carcinoma therapy in the future. Therefore, it is urgent to identify endogenous factors that control BLM gene expression for subsequent cancer therapy research.

MicroRNAs (miRNAs) are small, noncoding RNA molecules that inhibit gene expression by post-transcriptional interaction with the 3' untranslated region (3'-UTR) of target mRNAs. miRNAs are ~20 nucleotides in length and are highly conserved short single-stranded RNA molecules (15-17). Increasing evidence has revealed the critical roles of miRNAs in proliferation, colony formation, migration, invasion and DNA metabolism (18-20). miRNAs also have potential to be applied in cancer therapies as a novel drugs, and certain miRNAs that regulate BLM expression may be important for prostate carcinoma treatment. However, which miRNAs alter BLM helicase expression remains unclear. Recent studies have

suggested miRNAs are involved in proliferation, differentiation, invasion, migration, cell cycle and apoptosis by acting on BLM mRNA (21,22). Identifying miRNAs that target BLM is very useful and will expand the understanding of the relationship among miRNAs, BLM and cancer, as well as provide a prospective clinical treatment strategies for patients with prostate cancer by targeting BLM. However, one gene may be regulated by multiple miRNAs, so that the synergy or antagonism of miRNAs in post-transcriptional suppression process has huge potential benefits for novel miRNA and drug combination treatments. Therefore, understanding the miRNA interactions is important for further studies.

In the present study, prostate cancer cell line PC3 was selected for use in investigating the post-transcriptional regulation BLM gene expression by miRNA, and to understand whether potential anti-cancer drugs targeting BLM could be used in the future. Five miRNA were selected as candidates using online software and it was determined whether these have a negative effect on with BLM gene expression levels. miRNA mimics were overexpressed in PC3 cells and the BLM mRNA expression levels were subsequently detected. The miRNA seed sequence recognizes the target gene 3'-UTR, and a dual luciferase vector was constructed to detect miRNA effects on the target gene. Finally, western blot analysis was performed to monitor BLM protein expression levels following candidate miRNA overexpression. To determine the functional effects of multiple miRNAs in BLM gene expression, a Box-Behnken Design (BBD) experiment was designed to demonstrate the mutual effects between miRNAs. Proliferation, colony formation, migration and invasion assays provided further evidence for the hypothesis that miRNAs cooperatively regulate BLM gene expression and impact the normal proliferation and metabolism of cancer cells.

Materials and methods

miRNA screening. The tools, including miRSystem (mirsystem.cgm.ntu.edu.tw; version 21), TargetScan (www.targetscan.org; version 7.2), miRanda (www.microrna.org; version 2010), PicTar (www.pictar.org; version 2007), DIANA-MicroT-CDS (diana.imis.athena-innovation.gr; version 5.0), mirTarBase (mirtarbase.mbc.nctu.edu.tw; version 7.0) and DAVID (david.ncifcrf.gov; version 6.8), were used to identify miRNAs that potentially bind to the BLM 3'-UTR (Fig. 1). The TargetScan V7.2, mirTarBase and DAVID V6.8 had been jointly used to predict candidate roles in cells and further screen the potential that miRNAs regulate BLM expression. Finally, the five miRNAs were selected as candidates by logical estimate.

Cell culture and transfection. The human RWPE-2 normal prostate epithelial cell line and PC3 prostate cancer cell line were obtained from the Key Laboratory of Animal Genetics, Breeding and Reproduction (Guizhou University, Guiyang, China). RWPE-2 and PC3 were maintained using Dulbecco's modified Eagle's medium/F-12 medium (Gibco; Thermo Fisher Scientific, Inc., Waltham, MA, USA) in addition with 10% fetal bovine serum (Gibco; Thermo Fisher Scientific, Inc.) supplemented with 1% penicillin/streptomycin. Vector plasmids were constructed by a series of digestion and connection experiments. *Sal*I, *Xho*l and T4 ligase (Thermo Fisher Scientific, Inc.)

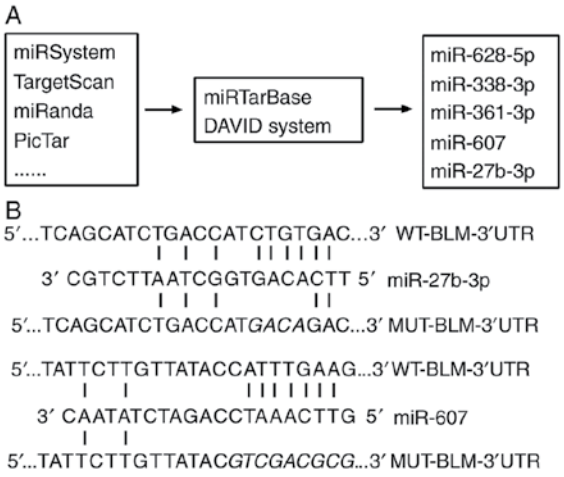

Figure 1. miR screening method and designed mutation or deletion sites. (A) Several prediction and function analysis software programs were used to screen candidate miRs, including miR-27b-3p, miR-607, miR-361-3p, miR-628-5p and miR-338-3p as candidates. (B) miR-27b-3p and miR-607 interaction sites with BLM 3'-UTR and mutational sites where four interaction bases of miR-27b-3p are changed and edited sequence where the interaction region of miR-607 is deleted. Predicted miR binding sites of BLM 3'-UTR are displayed. miR, microRNA; WT, wild type; BLM, BLM, BLM RecQ like helicase; UTR, untranslated region; MUT, mutated.

had were used within the process of vector construction. The constructed plasmids (Promega Corporation, Madison, WI, USA), and miRNA mimics (negative control; hsa-miR-27b-3p mimics; hsa-miR-607 mimics; hsa-miR-628-5p mimic; miR-338-3p mimic; hsa-miR-361-3p mimics; GenePharma Co., Ltd., Shanghai, China) were transfected into PC3 cells using Lipofectamine® 3000 (Invitrogen; Thermo Fisher Scientific, Inc.) when cells were ~60% confluent, with 2,500 ng plasmid and 5 μmol/l miRNA used per well of a 6-well-plate, according to the manufacturer's protocol. The transfection efficiency of miRNA mimics was monitored by reverse transcription-quantitative polymerase chain reaction (RT-qPCR) after 24 h.

RNA isolation and RT-qPCR. Total RNA was extracted by using TRIzol reagent (Thermo Fisher Scientific, Inc.) and RNA quality had been monitored by ultraviolet spectrophotometry (Thermo Fisher Scientific, Inc.). Designed stem-loop primers (23) and common primers, and 2 μg RNA were used for reverse transcription of miRNAs and BLM, respectively, using RevertAid First Strand cDNA Synthesis Kit (Thermo Fisher Scientific, Inc.). qPCR analyses were performed using CFX-96 Real-Time PCR Systems and SYBR Green Mix (Bio-Rad Laboratories, Inc., Hercules, CA, USA). Reverse and qPCR primers designed by software Primer5.0 and Oligo7.0 are shown in Tables I and II. miRNA transfectional efficiency is shown in Table III Relative expression levels were normalized to U6 or GAPDH, and calculated using the Pfaffl's method (calculated relative expression by using each PCR efficiency and of genes and Cq values).

$$\text{Ratio} = (1 + \text{E}_{\text{target}})^{\text{cq}_{\text{Tcontrol}} - \text{cq}_{\text{Tsample}}} (1 + \text{E}_{\text{reference}})^{\text{cq}_{\text{Rsample}} - \text{cq}_{\text{Rcontrol}}}$$

Ratio, relative expression ratio of target gene; Etarget, efficiency of target gene; Ereference, efficiency of reference gene; cqTsample, quantitative PCR cycle values of target gene in an unknown sample amplification satisfying

Table I. miR reverse primers.

Gene name	Sequence (5' to 3')
Stem loop sequence	GGTCGTATGCAAAGCAGGGTCCGAGGTATCCATCGCACGCATCGCACTGCATACGACC
RT-miR-27b-3p	GGTCGTATGCAAAGCAGGGTCCGAGGTATCCATCGCACGCATCGCACTGCA TACGACCGCAGAACTT
RT-miR-338-3p	GGTCGTATGCAAAGCAGGGTCCGAGGTATCCATCGCACGCATCGCACTGCATAC GACCCAACAAAATC
RT-miR-361-3p	GGTCGTATGCAAAGCAGGGTCCGAGGTATCCATCGCACGCATCGCACTGCATACGACC AAATCAGAATC
RT-miR-607	GGTCGTATGCAAAGCAGGGTCCGAGGTATCCATCGCACGCATCGCACTGCATACGAC CGTTATAGATCT
RT-miR-628-5p	GGTCGTATGCAAAGCAGGGTCCGAGGTATCCATCGCACGCATCGCACTGCATACGAC CCCTCTAGTAA
R-U6	AACGCTTCACGAATTTGCGT

Underlined indicates miRNA interaction sites in 3'-untranslated region. RT, reverse transcription; R, reverse; miR, microRNA.

Table II. Quantitative polymerase chain reaction primers.

Gene name	Amplified length (bp)	Sequence (5' to 3')
F-miR-27b-3p	76	GCGGCATTCACAGTGGCT
F-miR-338-3p	78	CGGCATCTCCAGCATCACT
F-miR-361-3p	77	CGGCATCCCCCAGGTGT
F-miR-607	78	CAGGCATCGTTCAAATCC
F-miR-628-5p	78	GGCGGCAATGCTGACATAT
miR-universal-R		CAAAGCAGGGTCCGAGGTATC
F-QBLM	245	AAGCGACATCAGGAGCCAAT
R-QBLM		GAAGAACTATCACCCCCCAGC
F-GAPDH	307	CGGAGTCAACGGATTTGGTCGTAT
R-GAPDH		AGCCTTCTCCATGGTGGTGAAGAC
F-U6	93	CTCGCTTCGGCAGCACA
R-U6		AACGCTTCACGAATTTGCGT

F, forward; miR, microRNA; R, reverse; BLM, BLM RecQ like helicase.

Table III. Transfectional efficiency detection of miR mimic.

miR	Fold increase vs. NC	P-value
miR-628-5p	360.21	P<0.001
miR-361-3p	4,802.11	P<0.001
miR-338-3p	36.147	P<0.001
miR-607	29,0972.79	P<0.001
miR-27b-3p	14.58	P<0.001

miR, microRNA.

the threshold; cqTcontrol, quantitative PCR cycle values of target gene in a control sample amplification satisfying the threshold; cqRsample, quantitative PCR cycle values of reference gene in an unknown sample amplification satisfying the threshold; cqRcontrol, quantitative PCR cycle values of reference gene in a control sample amplification satisfying the threshold.

Plasmids. The pmir-GLO dual luciferase reporter vector (Promega Corporation), which expresses Firefly and *Renilla* luciferase, was used for a reporter gene assay analyzing the potential targeting BLM region of miRNA. The BLM gene 3'-UTR, mutational and deleted fragments were amplified using designed primers (Table IV) for the PCR reaction and subcloned into the pmir-GLO dual luciferase reporter vector to obtained reporter vectors PGL-UTR-WT, PGL-UTR-MUT and PGL-UTR-DEL. All reconstruction vectors had been verified via enzyme digestion analysis and Sanger sequencing. Table IV displays relative amplification primers of fragments.

Table IV. Primers for fragment amplification.

Primer name	Amplified length (bp)	Sequence (5' to 3')
F-BLM-3'-UTR	264	CCGCTCGAGAAGCGACATCAGGAGCCAAT
R-BLM-3'-UTR		ACGCGTCGACGAAGAACTATCACCCCCCAGC
27b-mutation-F	113	CTGACCATGACAGACTATAAAGCTGTTAT
27b-mutation-R	173	CTTTATAGTCTGTCATGGTCAGATGCT
607-det-R	201	ACGCGTCGACGTATAACAAGAATA

F, forward; BLM, BLM RecQ like helicase; UTR, untranslated region; R, reverse.

Dual luciferase reporter assay. At 24 h after co-transfection with the miRNA mimic and constructed reporter vectors, PC3 cells were analyzed for luciferase activity using the Dual-Glo® Luciferase Assay kit (Promega Corporation) following manufacturer's protocol. PGL-UTR-WT and each miRNA were co-transfected into PC3 cells. PGL-UTR-MUT and miRNA (miR)-27b-3p, or PGL-UTR-DEL and miR-605 were co-transfected to further verify miRNA targeting sites of BLM. All data detected using a microplate reader are presented as relative firefly luciferase activity normalized to *Renilla* luciferase activity (Luc/Rluc).

Western blot analysis. Total proteins were extracted from cells using lysis buffer (Solarbio Science & Technology Co., Ltd., Beijing, China) containing protease inhibitors at 24 h post-transfection with the miRNA mimic. Protein concentration was determined using a BCA Protein Assay kit (Solarbio Science & Technology Co., Ltd.) and 10 mg of each protein sample was used for western blotting. Total protein had been stacked and separated by polyacrylamide gel electrophoresis by 6% stacking gel and 10% separating gel. Protein was transferred to PVDF (0.22 μm). The membrane was blocked using 5% defatted milk in TBS Tween (TBST) at 37˚C for 1.5 h. Specific monoclonal BLM (cat. no. ab5409; 1:1,000 dilution) and β-actin (cat. no. ab6276; 1:5,000 dilution) antibodies (Abcam, Cambridge, UK) in 5% defatted milk TBST were incubated with membranes at 4˚C for 12 h. Goat anti-mouse horseradish peroxidase-conjugated IgG (cat. no. ab97040) was used as the secondary antibody and incubated with the membrane at 37˚C for 1.5 h. When residual secondary antibodies were removed via TBST washing, the blot was detected using ImageLab software (version 2.0; Bio-Rad Laboratories, Inc.) after enzyme substrate reactions with BeyoECL Star Kit (Beyotime Institute of Biotechnology, Haimen, China).

BBD. In the present study, Box-Behnken factorial design including 17 runs, 3 factors and 3 levels had been applied to explore the interaction of miR-27b-3p and miR-607 in regulating BLM gene. The relative Luc/Rluc activities were detected at 24 h after miRNA and PGL-UTR-WT vector co-transfection into PC3 and were used to calculate the interaction effects between miRNAs using Design-Expert 8.0 software (Stat-Ease, Inc., Minneapolis, MN, USA). Designed doses of miRNAs and designed methods were displayed in tables and each factor was coded by three levels: Low (-1; 0 μmol/l), medium (0; 5 μmol/l) and high (+1; 10 μmol/l; Tables V and VI).

Table V. Coded and real values of variables in the Box-Behnken design.

		Level (μmol/l)		
Symbol	Variable	-1	0	+1
A	miR-607	0	5	10
B	miR-27b-3p	0	5	10
C	miR-338-3p	0	5	10

Table VI. Box-Behnken design with code values.

Experiment number	A, miR-607	B, miR-27b-3p	C, miR-338-3p
1	-1	-1	0
2	1	-1	0
3	-1	1	0
4	1	1	0
5	-1	0	-1
6	1	0	-1
7	-1	0	1
8	1	0	1
9	0	-1	-1
10	0	1	-1
11	0	-1	1
12	0	1	1
13	0	0	0
14	0	0	0
15	0	0	0
16	0	0	0
17	0	0	0

Cell proliferation and colony formation assays. Cell proliferation was measured using the MTT method. Cells were seeded (10,000 cells/well), transfected with 2.5 μmol/l miRNA mimic in 12-well plates and incubated for various times. MTT incubation for 4 h, DMSO added to dissolve formazan, medium was removed and sample absorbency was detected at 490 nm. The growth curves over 3 days were calculated using the mean

values of four wells. In the colony formation assay, PC3 cells transfected with miRNA were seeded at 5,000 cells/well in 12-well-plates and cell colonies in each well were counted following Giemsa staining after 5 days. Methanol (100%) was used to fix cells for 10 min at room temperature before Giemsa staining (1 mg/ml) for 10 min at room temperature. The numbers of colonies were counted using Gel-Pro32 software (version 4.0; Media Cybernetics, Inc., Rockville, MD, USA).

Cell invasion and migration assays. Transwell chambers (Corning Inc., Corning, NY, USA) where the two chambers were separated by a Matrigel-coated polycarbonate membrane (Solarbio Science & Technology Co., Ltd.; size: 8 μm) were used to analyze cell invasion at 12 h after transfection. The upper chamber was filled with serum-free medium and the lower chamber was filled with complete medium with 10% FBS. Cells (5,000 per well) were added into the upper chamber and invaded cells were counted after 12 h. Cells were stained with 0.1% crystal violet for 15 min at room temperature after 4% paraformaldehyde fixation for 10 min in the lower chamber. Cell migration was monitored via wound healing assay and Transwell chamber assays. Briefly, when transfected cells were 80-90% confluent, a wound was created using a pipette tip and the heal distance was recorded after 24 h to study cell migration ability. Cell migration was also analyzed using a Transwell chamber without Matrigel coating. Harvested cells (5,000 per well) were added into the upper chamber with serum-free medium and the lower upper chamber was filled with 10% FBS medium. Invaded cells in the lower chamber were stained with 0.1% crystal violet for 15 min at room temperature after 4% paraformaldehyde fixation for 10 min after 12 h to analyze cell migration.

Statistical analysis. Statistical analysis was performed using SPSS software (version 22.0; IBM, Corp., Armonk, NY, USA), and the BBD experiment was designed and analyzed using Design-Expert software (version 8.0; Stat-Ease, Inc.). Data is presented as the mean ± standard deviation. The difference between two experimental groups and multiple comparisons were analyzed by Student's t-test (two-tailed and equal variance) and Tukey's honestly significant difference method following ANOVA, respectively. $P<0.05$ was considered to indicate a statistically significant differences.

Results

Screen of miRNAs targeting BLM. According published researches (18-20) and bioinformatics analysis, five candidate miRNAs, miR-27b-3p, miR-607, miR-338-3p, miR-361-3p and miR-628-5p, were identified using TargetScan, miRanda, DIANA and others. miRNA function prediction was analyzed using the DAVID system (the technological process is presented in Fig. 1A). Furthermore, the expression levels of miRNAs in PC3 and RWPE-2 cell lines were detected to determine the association between miRNAs and BLM expression, which demonstrated that miR-338-3p and miR-607 had a similar expression pattern to BLM gene in cancer cells and normal cells, whereas miR-628-5p, miR-361-3p and miR-27b-3p the opposite pattern of expression (Fig. 2). The effects of miRNA overexpression on BLM in PC3 cells were analyzed at 24 and 48 h after transfection (Fig. 3). The results demonstrated that miR-338-3p and miR-607 decreased BLM gene expression in mRNA levels at 24 h, although the decrease was not statistically significant. However, miR-338-3p transfection for 48 h significantly increased BLM mRNA levels in PC3 cells ($P<0.01$). Additionally, miR-607 significantly decreased BLM mRNA expression at 48 h after transfection ($P<0.01$). Other miRNAs had no significant effects on BLM mRNA expression compared with the NC group ($P>0.05$). Dual luciferase activity was determined following co-transfection of PC3 cells with miRNA and PGL-UTR-WT containing the wild type 3'-UTR of BLM. miR-607 and miR-27b-3p modulated BLM gene relative luciferase activity by directly targeting the BLM 3'-UTR (Fig. 4A).

Validation of the effects of miR-607 and miR-27b-3p. Following the initial results, for investigation of the regulatory roles of miR-607 and miR-27b-3p, PGL-UTR-MUT, in which four key bases were mutated at the miR-27b-3p binding sites, and PGL-UTR-DEL, in which miR-607 binding sites in the BLM 3'-UTR was deleted, were used for further validation. The designed mutation and deletion sites are presented in on Fig. 1B. PC3 cells were co-transfected with PGL-UTR-MUT or PGL-UTR-DEL and miR-27b-3p or miR-607, respectively, and relative luciferase activity was measured after 24 h (Fig. 4B). PGL-UTR-WT co-transfection with miR-27b-3p or miR-607 decreased luciferase activity compared with PGL-UTR-WT transfection alone ($P<0.05$ and $P<0.01$, respectively), whereas PGL-UTR-MUT co-transfection with miR-27b-3p, and PGL-UTR-DEL co-transfection with miR-607 produced no significant difference compared the vector control ($P>0.05$). Finally, BLM helicase expression was determined by western blot analysis after miR-27b-3p and miR-607 overexpression in PC3 cells. miR-27b-3p and miR-607 reduced BLM helicase protein expression compared with NC mimic transfection (Fig. 5).

Interaction between miRNAs. BBD was applied to explore interactions between miRNAs. In the previous assays, miR-338-3p had the activity to impair relative luciferase and displayed a multiple effects in various acting doses or times. Therefore, miR-338-3p was selected as one factor to represent endogenous noise of miRNAs. The relative luciferase activity of all runs including different miRNA dose compositions is presented in Table VII. The final results are presented in Table VIII, which demonstrated that the calculated statistical model is statistically significant ($P<0.01$) and the lack of fix is not significant ($P>0.8$). It indicated that a proper formula mode had been built for prediction of interaction effects between miRNAs on the luciferase activity of PGL-UTR-WT containing the BLM 3'-UTR. miR-27b-3p and miR-607 were significant factors ($P<0.01$) affecting relative luciferase activity, but the effect of miR-338-3p on relative luciferase activity was not significant ($P>0.05$). The results also demonstrated that the interaction effects between miR-607 and miR-27b-3p, and interaction effects between miR-607 and miR-338-3p were statistically significant ($P<0.05$), but the interaction effect of miR-27b-3p and miR-338-3p was not significant ($P>0.05$). The calculated model coefficient is presented in Table IX, and the negative values of factors by code value calculation suggested a decrease in relative luciferase activity. Thus, the calculated equation indicated the synergetic inhibitory effects of miR-607, and miR-27b-3p or miR-338-3p. The radian degree and direction of curves on contours in Fig. 6

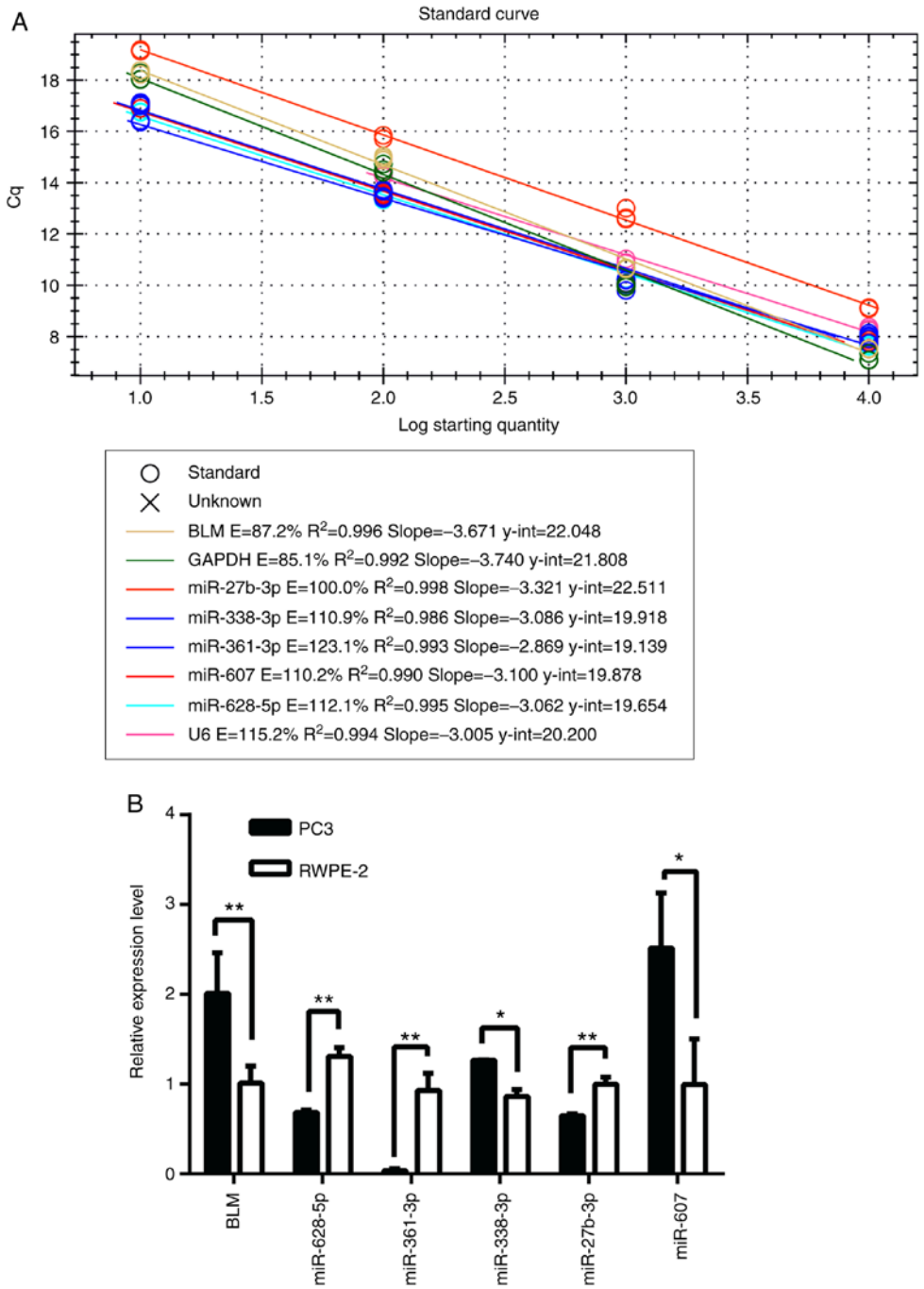

Figure 2. Amplification efficiencies and expression levels of BLM mRNA and five miRNAs in RWPE-2 and PC3 cell lines. BLM, miR-628-5p, miR-361-3p, miR-338-3p, miR-27b-3p and miR-607 expression was analyzed by reverse transcription-quantitative polymerase chain reaction and (A) standard curve equations of amplification are shown. (B) The relative mRNA and miRNA expression levels were normalized to GAPDH and U6 respectively and following Pfaffl's method was applied to calculate expression levels. n=3. *P<0.05, **P<0.01. BLM, BLM, BLM RecQ like helicase; miR, microRNA.

demonstrated the intensity and manner of interactions between two factors in different dose compositions. The interactional contour between miR-607 and miR-27b-3p further demonstrated their synergistic effects on the reduced BLM gene expression.

Effects of miR-27b-3p and miR-607 on PC3 proliferation, colony formation, migration and invasion. The effects of miR-27b-3p and miR-607 on PC3 cell proliferation (Fig. 7), colony formation (Fig. 8), migration (Fig. 9) and invasion (Fig. 10) were analyzed. All results are summarized in Table X, which demonstrated that miR-27b-3p overexpression in PC3 cells reduces proliferation, colony formation and invasion abilities compared with the NC group (P<0.01). miR-607 overexpression significantly reduced colony formation and migration of PC3 cells (P<0.01).

Discussion

In the current study, five miRNAs were identified using various online software tools, and miR-27b-3p and miR-607 were validated suppressors of BLM gene expression (19). The different online software varying featured that were considered

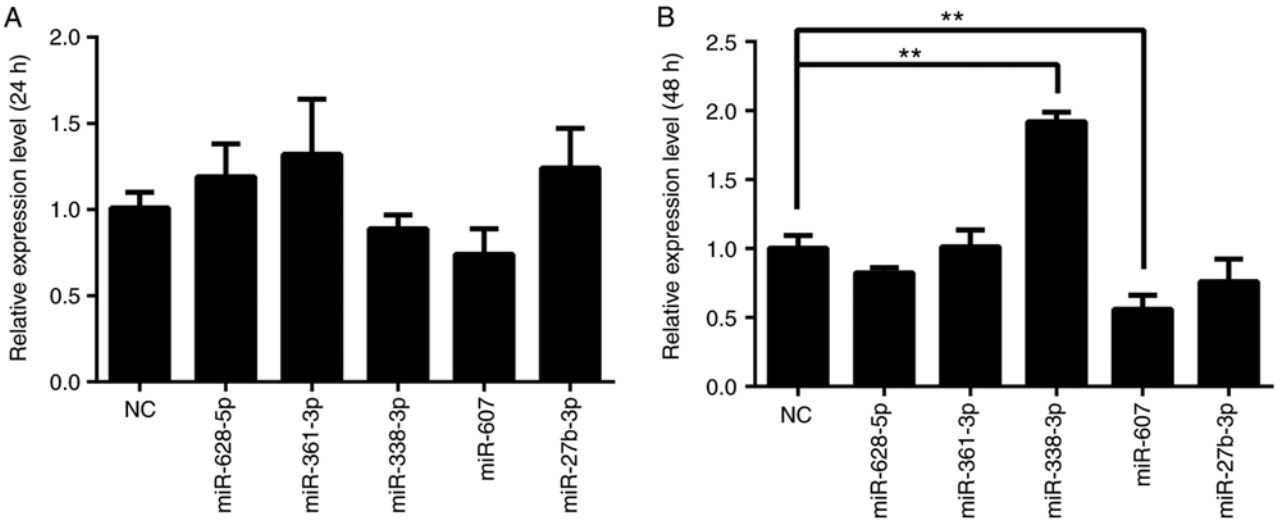

Figure 3. BLM gene expression levels in mRNA levels after miRs overexpression. PC3 cells transfected with miR mimic and samples were collected and analyzed by reverse transcription-quantitative polymerase chain reaction at (A) 24 and (B) 48 h. BLM gene expression was normalized to GAPDH. n=3. **P<0.01. BLM, BLM RecQ like helicase; NC, negative control; miR, microRNA.

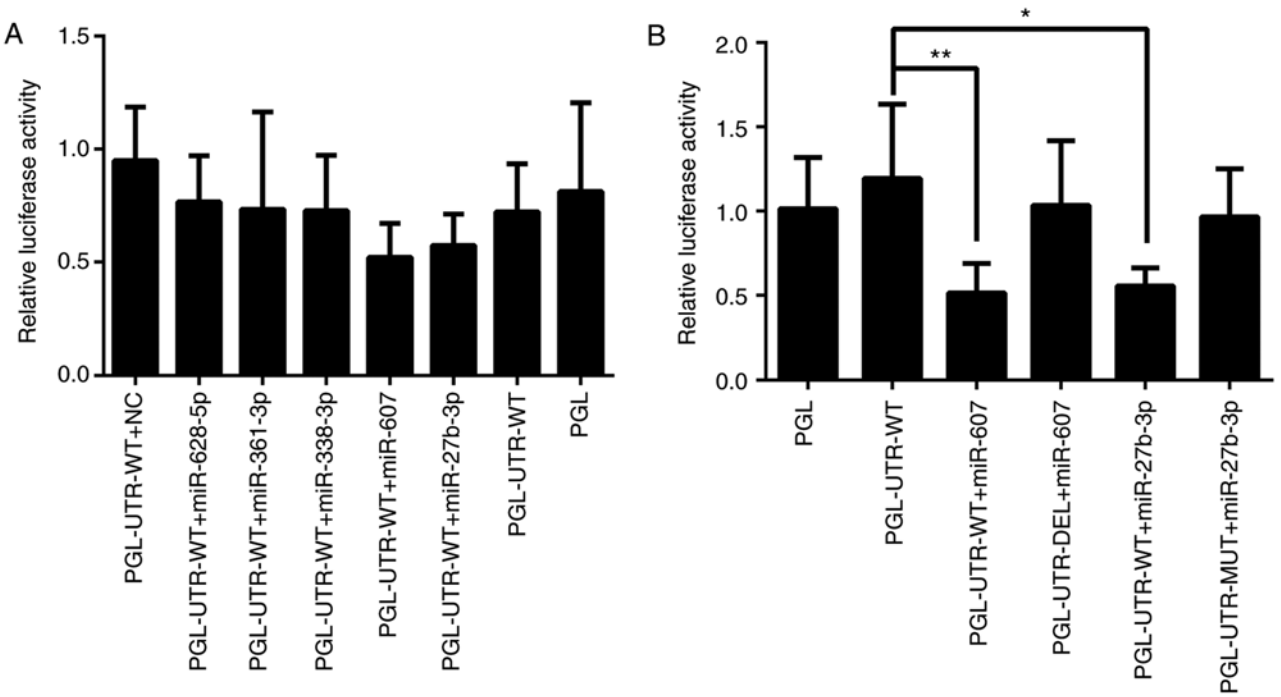

Figure 4. Effects of miRs on relative luciferase activity. PC3 cells were co-transfected with miR mimic and luciferase reporter vectors. Relative luciferase activity was detected at 24 h and the firefly luciferase activity of each sample was normalized to the *Renilla* luciferase activity. PGL-UTR-WT is a reporter vector containing the wild 3'-UTR sequence BLM mRNA at the 3'-terminal of the firefly luciferase sequence in the pmir-GLO vector. Similarly, PGL-UTR-MUT is a reporter vector containing a mutated BLM 3'-UTR containing an miR-27b-3p interaction region (changed at four bases). PGL-UTR-DEL is a reporter vector with the BLM 3'-UTR sequence containing a miR-607 interaction region partially deleted. (A) Relative luciferase activity results of PGL-UTR-WT + miR mimics. (B) Relative luciferase activity of PGL-UTR-MUT or PGL-UTR-DEL + miR mimics. n=6. *P<0.05, **P<0.01. BLM, BLM RecQ like helicase; PGL, pmir-GLO; UTR, untranslated region; WT, wild-type; NC, negative control; miR, microRNA; DEL, deletion; MUT, mutation.

to identify the most potential miRNAs for subsequent validation *in vitro*. Bioinformatics selection (data not shown) identified miR-628-5p, miR-361-3p, miR-338-3p, miR-607 and miR-27b-3p as potential candidate miRs that may target BLM mRNA. Recent studies indicated that miR-361-3p, miR-338-3p and miR-27b-3p have oncosuppressive functions. There are fewer studies on miR-607 (24) and miR-628-5p (25) so further study is required. Subsequently, the expression of the five miRNAs and BLM were detected by RT-qPCR in normal cells (RWPE-2 cell line) and a cancer cell line (PC3) to determine the expression correlation between these miRNAs and BLM. The results indicated that miR-628-5p, miR-361-3p and miR-27b-3p had lower expression in PC3 cells than in RWPE-2 cells, whereas BLM, miR-338-3p and miR-607 had the opposite pattern of expression. The negative association between BLM gene expression, and miR-628-5p, miR-361-3p

Table VII. Results of BBD for relative Luc/Rluc activity.

Experiment number	A, miR-607	B, miR-27b-3p	C, miR-338-3p	Relative Luc/Rluc activity (%)
1	-1	-1	0	84.74
2	1	-1	0	80.42
3	-1	1	0	77.5
4	1	1	0	53.38
5	-1	0	-1	74.44
6	1	0	-1	74.55
7	-1	0	1	83.25
8	1	0	1	63.02
9	0	-1	-1	81.61
10	0	1	-1	73.81
11	0	-1	1	75.6
12	0	1	1	64.61
13	0	0	0	70.44
14	0	0	0	69.9
15	0	0	0	68.86
16	0	0	0	81.05
17	0	0	0	71.08

Designed BBD experiment runs and their respective response results. BBD, Box-Behnken design; Luc/Rluc, luciferase/*Renilla* luciferase; miR, microRNA.

Table VIII. Results of statistics for Box-Behnken design.

Source	Sum of squares	df	Mean square	F-value	P-value (Prob >F)
Model	890.82	6	148.47	8.89	0.0016
A (miR-607)	294.76	1	294.76	17.65	0.0018
B (miR-27b-3p)	352.00	1	352.00	21.08	0.0010
C (miR-338-3p)	40.16	1	40.16	2.41	0.1520
AB	97.98	1	97.98	5.87	0.0359
AC	103.38	1	103.38	6.19	0.0321
BC	2.54	1	2.54	0.15	0.7048
Residual	166.96	10	16.70		
Lack of fit	67.81	6	11.30	0.46	0.8137
Pure error	99.15	4	24.79		
Cor total	1057.78	16			

df, degrees of freedom; miR, microRNA.

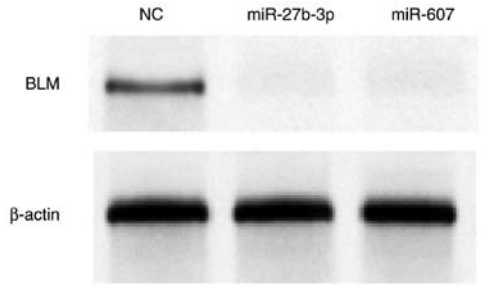

Figure 5. Western blot analysis of BLM protein expression levels in PC3 cells at 24 h after miR or NC mimic transfection. NC, negative control; miR, microRNA; BLM, BLM RecQ like helicase.

and miR-27b-3p levels suggested that miR-628-5p, miR-361-3p and miR-27b-3p may be potential miRNAs that regulate BLM gene expression at the post-transcriptional level. The results of the dual luciferase assay and western blot analysis revealed that miR-27b-3p and miR-607 inhibit BLM gene expression. Additionally, previous studies have indicated that miR-628-5p, miR-361-3p and miR-27b-3p may be anti-cancer factors, as they have lower expression levels in cancer compared with normal cells (18,26,27). However, more tumor samples and cell lines are required to determine whether these miRNAs are anti-cancer factors. By contrast, the higher expression level of BLM, miR-338-3p and miR-607 in PC3 cells indicate that

Table IX. Predicted equation by Box-Behnken design in code value.

Coefficient factor	Standard estimate	df	Error	95% CI (low)	95% CI (high)	VIF
Intercept	73.43	1	0.99	71.22	75.64	
A (miR-607)	-6.07	1	1.44	-9.29	-2.85	1.00
B (miR-27b-3p)	-6.63	1	1.44	-9.85	-3.41	1.00
C (miR-338-3p)	-2.24	1	1.44	-5.46	0.98	1.00
AB	-4.95	1	2.04	-9.50	-0.40	1.00
AC	-5.08	1	2.04	-9.64	-0.53	1.00
BC	-0.80	1	2.04	-5.35	3.76	1.00

Negative value indicates positive action on BLM expression inhibition. df, degrees of freedom; CI, confidence interval; miR, microRNA; VIF, variance inflation factor.

Table X. Effect of miRs on PC3 cells.

miR	Proliferation	Colony formation	Migration (cell scratch)	Migration (transwell)	Invasion (transwell)
miR-27b-3p	-[a]	-[a]			-[a]
miR-607		-[a]	-[a]	-[b]	

-, miR can decrease relative ability; [a]P<0.01, [b]P<0.05 vs. control group. miR, microRNA.

they may have the potential to be tumor markers for clinical diagnosis (21,28). miRNA overexpression, dual luciferase assays and western blot analysis were performed to explore the role of these miRNAs in the regulation of BLM. The results indicated that miR-607 and miR-338-3p decreased the level of BLM mRNA at 24 h post-transfection, whereas miR-338-3p elevated the BLM mRNA level at 48 h post-transfection. miR-607 significantly reduced the BLM mRNA level at 48 h post-transfection, but miR-27b-3p had no evident effect on BLM mRNA. However, the dual luciferase assay and western blot results suggested that miR-27b-3p and miR-607 can target the BLM 3'-UTR reduce the protein expression. This suggested that miR-607 and miR-27b-3p act by decreasing BLM mRNA levels and reducing the translation of BLM mRNA, respectively.

Multiple mechanisms of action of miRNAs allow for positive or negative mutual effect between miRNAs. Mutual effect of miRNAs may have many advantages for medicinal application, such as higher drug efficacy and lower secondary actions (29,30). Understanding the interaction mechanisms of miRNAs provides more information on the regulation process of BLM gene expression at the post-transcriptional level. BBD has been applied to determine interactions between multiple factors in previous studies (31). Latin square design and the equivalent line method (2,30-32) are also able to calculate interaction effects, but the lower dose application of factors, more reasonable and three-dimensional arrangements are the main features of BBD which eliminates the dose superposing effects from multiple factors (in the study of factor interaction, multiple factors were used in one treatment group so that the dose of multiple factors will be elevated to create effect results). By contrast, Latin square design lacks consideration of superposition of drug doses. Higher doses will lead to more errors from random and toxic effects, but lower dose will lose effects, which can be resolved using a BBD experiment. A parabolic dose-effect curve is necessary for the equivalent line method and two dose-effect curves of drugs must not cross. In brief, BBD was the best choice for analyzing the interaction effects among the miRNAs in the present study. miR-27b-3p and miR-607 were demonstrated to reduce BLM protein expression, and understanding their mutual effects has potential to assist future drug development. miR-338-3p has been reported to influence the proliferation and metabolism of cancer cells in recent reports (19,33). According to our findings, action time and dose altered the effects of miR-338-3p on BLM mRNA levels, which implied miR-338-3p may be selected as a reference factor which represents other functional miRNAs in PC3 cells to research miRNA interactions in depth. Therefore, miR-338-3p is suitable to be selected as a factor that represents endogenous miRNAs noise to explore interaction effects between miR-27b-3p and miR-607. miR-338-3p had been selected as auxiliary miRNA to analyze the interaction between miR-27b-3p and miR-607 for a deeper understating of the effects of multiple miRNA interactions on BLM expression. It was demonstrated that the interaction between miR-27b-3p with miR-607, and the interaction between miR-338-3p and miR-607 decreased relative luciferase activity of the BLM reporter, but there was no interaction between miR-27b-3p and miR-338-3p. This indicated that miR-27b-3p and miR-338-3p have the same action mode, so that they have no distinct interaction; whereas, the different action modes between miR-607 and miR-27b-3p created a synergistic effect between miR-27b-3p and miR-607 on the expression suppression of BLM. miR-607 overexpression in

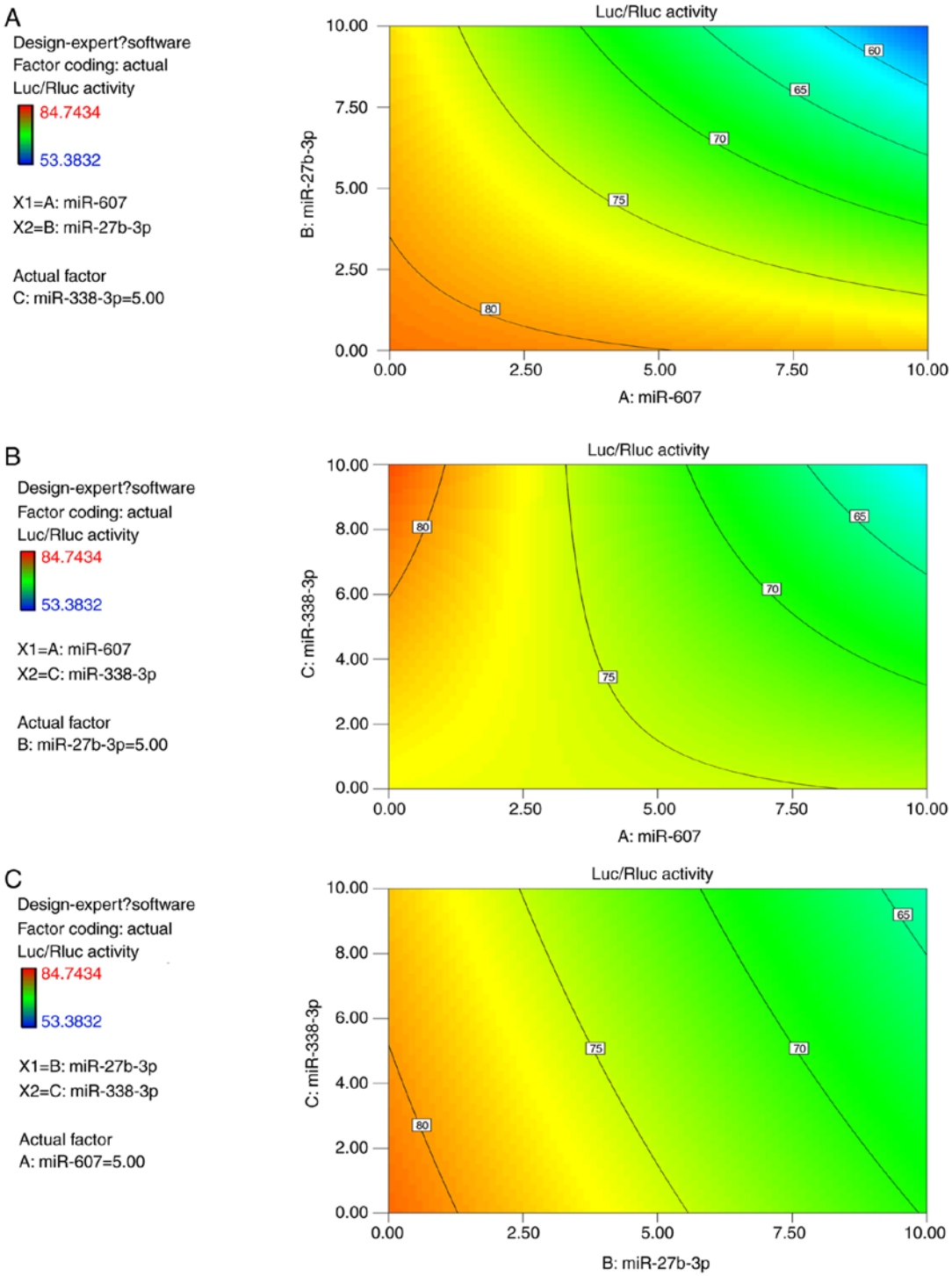

Figure 6. Response surface contour map. PGL-UTR-WT and different doses of miR-27b-3p, miR-607 and miR-338-3p were co-transfected into PC3 cells. The relative luciferase activity was detected to determine interactions among miRs targeting BLM. The contour map shows the 0 dose levels (5 μmol/l) of each miR to ease understanding of the interaction effect between miRs. (A) Interaction contour map between miR-27b-3p and miR-607 where the 0 dose level of miR-338-3p has been applied. (B) Interaction contour map between miR-338-3p and miR-607 where the 0 dose level of miR-27b-3p has been applied. (C) Interaction contour map between miR-27b-3p and miR-338-3p where the 0 dose level of miR-607 has been applied. n=6. PGL, pmir-GLO; UTR, untranslated region; WT, wild-type; Luc/Rluc, luciferase/*Renilla* luciferase; miR, microRNA.

PC3 resulted in reduced BLM mRNA level, but miR-27b-3p did not reduce the mRNA level, which also had supported the hypothesis of synergistic effects between miR-27b-3p and miR-607 via different mechanisms of action.

In previous studies, miR-27b-3p (22) and miR-607 (34) were to have anti-cancer functions. It was indicated that miR-27b-3p and miR-607 alter normal proliferation, invasion and migration of prostate cancer cells by decreasing BLM protein expression. Additionally, the effects of miR-27b-3p and miR-607 on the proliferation, migration, invasion and colony formation of PC3 cells were determined. miRNAs regulate important protein expression to alter various cell functions, although the detail mechanisms of the roles of miR-27b-3p and miR-607 in PC3 cells remain unknown as miRNAs commonly regulate

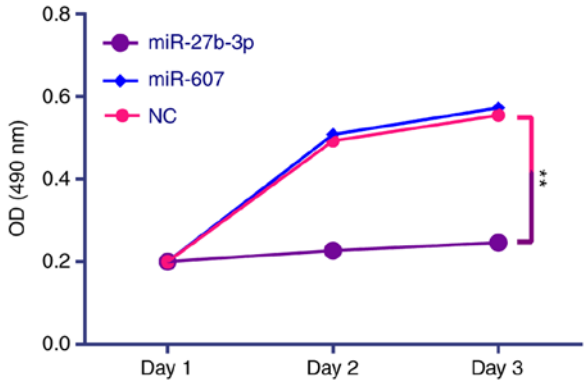

Figure 7. Effects of miR on PC3 cell proliferation. PC3 cells were collected following transfection with miR-27b-3p, miR-607 or NC mimics and used to analyze cell proliferation in an MTT assay. n=4. **P<0.01. OD, optical density; miR, microRNA; NC, negative control.

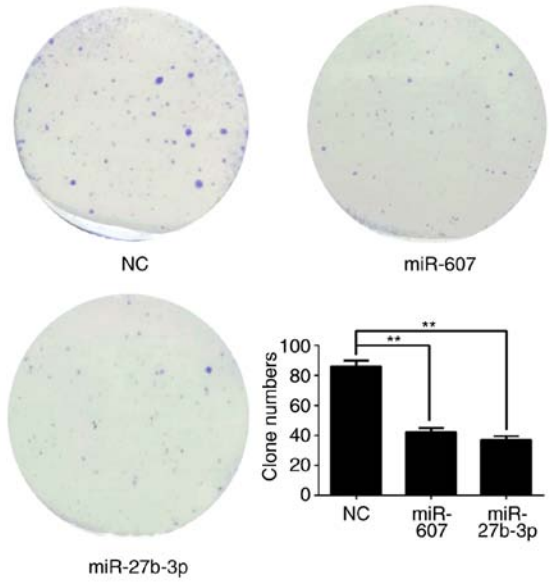

Figure 8. Effects of miR on colony formation of PC3 cells. The number of cell colonies was determined after 5 days of inoculation of PC3 cells in 12-well plates during colony formation assay. **P<0.01. NC, negative control; miR, microRNA.

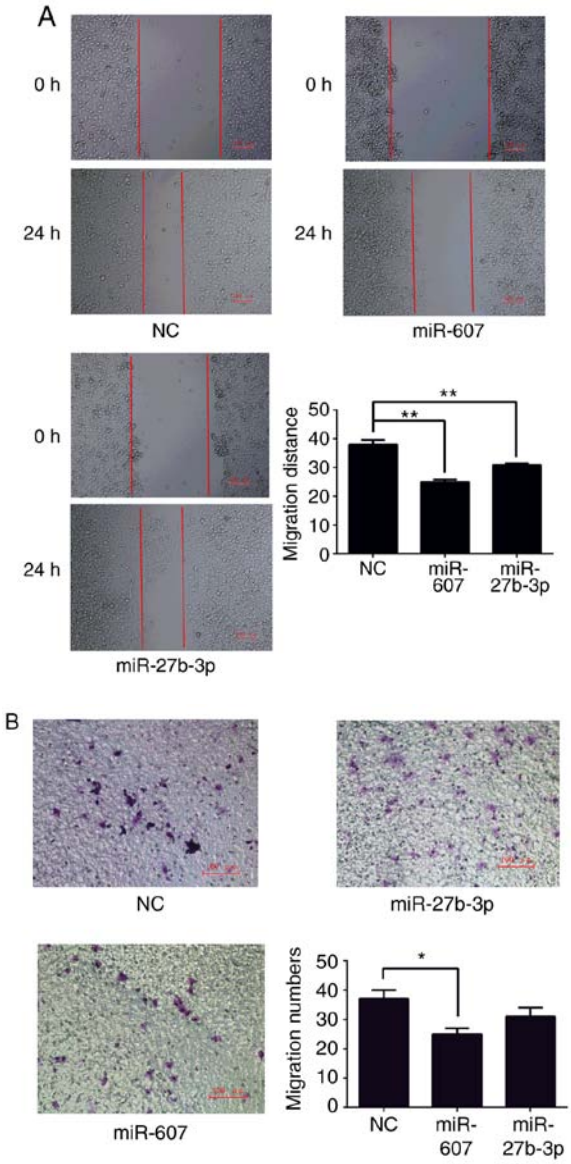

Figure 9. Cell migration assays. (A) Wound healing (n=3) and (B) Transwell chambers assays (five fields of view; n=3) were performed to detect migration of PC3 cells post-transfection with miR or NC mimic. *P<0.05, **P<0.01. NC, negative control; miR, microRNA.

multiple target genes, and a gene is also regulated by multiple miRNAs (17). The current study demonstrated that miR-27b-3p and miR-607 cooperatively affected PC3 cells by directly targeting the BLM gene 3'-UTR to have tumor-inhibiting functions. Previous research demonstrated that ML216, which is a small molecule inhibitor of BLM, has anti-proliferative activity in cells (9,35), and BLM defects also increase the sensitivity of cancer cells to cytotoxic drugs (36). Thus, the effects of miRNAs on the proliferation, migration, invasion and colony formation of PC3 cells was analyz ed to provide the evidence and theoretical support for clinical treatment of prostate cancer using miRNAs to inhibit BLM pathways. However, expression levels of key protein factors, such as matrix metalloproteinases, cadherins, vascular endothelial growth factor, catenin, need to be determined for stronger evidence.

Finally, it was validated that miR-27b-3p and miR-607 cooperatively reduce BLM gene expression by directly

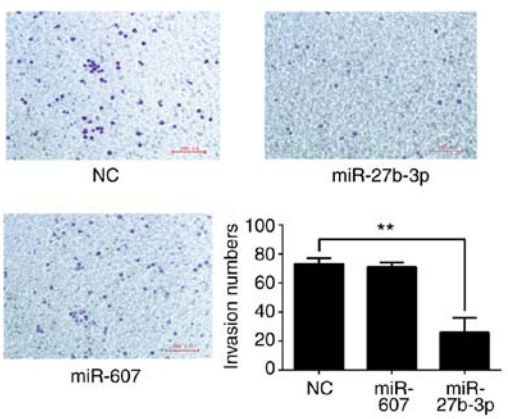

Figure 10. Cell invasion assays. Transwell chambers assays (five fields of view; n=3) were used to detect invasion of PC3 cells post-transfection with miR or NC mimic. The relative histogram results were represented. **P<0.01. NC, negative control; miR, microRNA.

targeting gene the BLM 3'-UTR in PC3 cells and provided information on the post-transcriptional regulation of BLM gene expression. The synergistic use of miR-27b-3p and miR-607 to target BLM gene was more effective than their use alone. In conclusion, the presented study provided evidence that miR-27b-3p and miR-607 have anti-cancer activity, and cooperatively downregulate BLM expression at the post transcriptional level in PC3 cells.

BLM helicase is crucial factor required cell DNA metabolism and is involved in cell proliferation, migration, invasion, apoptosis and the cell cycle in prostate cancer cells (5). Prostate cancer is the second leading cause of cancer-associated mortality in men (1). Targeting the key protein factors, such as BLM, Her2/Neu, epidermal growth factor or tumor necrosis factor-α, in cancer cells by anticancer drugs is main and valid method for cancer remedy (3,5). Targeting BLM helicase may be a useful future method to treat patients with prostate cancer (5). However, the post-transcription regulation of BLM gene has remained unclear, which has limited the application and development of drugs targeting BLM helicase. It is important to explore novel anti-cancer drugs targeting BLM, to understand the BLM gene regulation pathway and to identify other novel cancer targets and tumor markers.

Acknowledgements

This work was supported by the Key Laboratory of Animal Genetics, Breeding and Reproduction in Guizhou Province (Guiyang, China). We thank Dr Chen Kun of Guizhou Provincial People's Hospital (Guiyang, China) for providing the RWPE-2 cell line and the expert technical assistance of Professor He Laping (School of Liquor and Food Engineering, Guizhou University).

Funding

Funding was provided by the Natural Science Foundation of China (grant no. 31361406).

Availability of data and materials

The datasets used and/or analyzed during the current study are available from the corresponding author on reasonable request.

Authors' contributions

YC designed the study, performed the research, analyzed data and wrote the paper. HX and TG helped design the study and checked the data. JZ and SW helped perform research and analyzed data. ZD and WC helped designed the study and analyzed data.

Ethics approval and consent to participate

Not applicable.

Patient consent for publication

Not applicable.

Competing interests

The authors declare that they have no competing interests.

References

1. Torre LA, Bray F, Siegel RL, Ferlay J, Lortet-Tieulent J and Jemal A: Global cancer statistics, 2012. CA Cancer J Clin 65: 87-108, 2015.
2. Pandita A, Manvati S, Singh SK, Vaishnavi S and Bamezai RN: Combined effect of microRNA, nutraceuticals and drug on pancreatic cancer cell lines. Chem Biol Interact 233: 56-64, 2015.
3. Shi S, Han L, Deng L, Zhang Y, Shen H, Gong T, Zhang Z and Sun X: Dual drugs (microRNA-34a and paclitaxel)-loaded functional solid lipid nanoparticles for synergistic cancer cell suppression. J Control Release 194: 228-237, 2014.
4. Futami K, Ogasawara S, Goto H, Yano H and Furuichi Y: RecQL1 DNA repair helicase: A potential tumor marker and therapeutic target against hepatocellular carcinoma. Int J Mol Med 25: 537-545, 2010.
5. Qian X, Feng S, Xie D, Feng D, Jiang Y and Zhang X: RecQ helicase BLM regulates prostate cancer cell proliferation and apoptosis. Oncol Lett 14: 4206-4212, 2017.
6. Bachrati CZ and Hickson ID: RecQ helicases: Suppressors of tumorigenesis and premature aging. Biochem J 374: 577-606, 2003.
7. Sharma S, Doherty KM and Brosh RM Jr: Mechanisms of RecQ helicases in pathways of DNA metabolism and maintenance of genomic stability. Biochem J 398: 319-337, 2006.
8. Wu L: Role of the BLM helicase in replication fork management. DNA Repair (Amst) 6: 936-944, 2007.
9. Nguyen GH, Dexheimer TS, Rosenthal AS, Chu WK, Singh DK, Mosedale G, Bachrati CZ, Schultz L, Sakurai M, Savitsky P, *et al*: A small molecule inhibitor of the BLM helicase modulates chromosome stability in human cells. Chem Biol 20: 55-62, 2013.
10. Laitman Y, Boker-Keinan L, Berkenstadt M, Liphsitz I, Weissglas-Volkov D, Ries-Levavi L, Sarouk I, Pras E and Friedman E: The risk for developing cancer in Israeli ATM, BLM, and FANCC heterozygous mutation carriers. Cancer Genet 209: 70-74, 2016.
11. de Voer RM, Hahn MM, Mensenkamp AR, Hoischen A, Gilissen C, Henkes A, Spruijt L, van Zelst-Stams WA, Kets CM, Verwiel ET, *et al*: Deleterious germline BLM mutations and the risk for early-onset colorectal cancer. Sci Rep 5: 14060, 2015.
12. Böhm S and Bernstein KA: The role of post-translational modifications in fine-tuning BLM helicase function during DNA repair. DNA Repair (Amst) 22: 123-132, 2014.
13. Suspitsin EN, Yanus GA, Sokolenko AP, Yatsuk OS, Zaitseva OA, Bessonov AA, Ivantsov AO, Heinstein VA, Klimashevskiy VF, Togo AV and Imyanitov EN: Development of breast tumors in CHEK2, NBN/NBS1 and BLM mutation carriers does not commonly involve somatic inactivation of the wild-type allele. Med Oncol 31: 828, 2014.
14. Sassi A, Popielarski M, Synowiec E, Morawiec Z and Wozniak K: BLM and RAD51 genes polymorphism and susceptibility to breast cancer. Pathol Oncol Res 19: 451-459, 2013.
15. Matsuyama R, Okuzaki D, Okada M and Oneyama C: MicroRNA-27b suppresses tumor progression by regulating ARFGEF1 and focal adhesion signaling. Cancer Sci 107: 28-35, 2016.
16. Wen C, Liu X, Ma H, Zhang W and Li H: miR-338-3p suppresses tumor growth of ovarian epithelial carcinoma by targeting Runx2. Int J Oncol 46: 2277-2285, 2015.
17. Filipowicz W, Bhattacharyya SN and Sonenberg N: Mechanisms of post-transcriptional regulation by microRNAs: Are the answers in sight? Nat Rev Genet 9: 102-114, 2008.
18. Chen D, Si W, Shen J, Du C, Lou W, Bao C, Zheng H, Pan J, Zhong G, Xu L, *et al*: miR-27b-3p inhibits proliferation and potentially reverses multi-chemoresistance by targeting CBLB/GRB2 in breast cancer cells. Cell Death Dis 9: 188, 2018.
19. Sui GQ, Fei D, Guo F, Zhen X, Luo Q, Yin S and Wang H: MicroRNA-338-3p inhibits thyroid cancer progression through targeting AKT3. Am J Cancer Res 7: 1177-1187, 2017.
20. Hara ES, Ono M, Eguchi T, Kubota S, Pham HT, Sonoyama W, Tajima S, Takigawa M, Calderwood SK and Kuboki T: miRNA-720 controls stem cell phenotype, proliferation and differentiation of human dental pulp cells. PLoS One 8: e83545, 2013.

21. Xu S, Yi XM, Zhang ZY, Ge JP and Zhou WQ: miR-129 predicts prognosis and inhibits cell growth in human prostate carcinoma. Mol Med Rep 14: 5025-5032, 2016.
22. Zhang G, Tian X, Li Y, Wang Z, Li X and Zhu C: miR-27b and miR-34a enhance docetaxel sensitivity of prostate cancer cells through inhibiting epithelial-to-mesenchymal transition by targeting ZEB1. Biomed Pharmacother 97: 736-744, 2018.
23. Chen C, Ridzon DA, Broomer AJ, Zhou Z, Lee DH, Nguyen JT, Barbisin M, Xu NL, Mahuvakar VR, Andersen MR, *et al*: Real-time quantification of microRNAs by stem-loop RT-PCR. Nucleic Acids Res 33: e179, 2005.
24. Braoudaki M, Lambrou GI, Giannikou K, Milionis V, Stefanaki K, Birks DK, Prodromou N, Kolialexi A, Kattamis A, Spiliopoulou CA, *et al*: Microrna expression signatures predict patient progression and disease outcome in pediatric embryonal central nervous system neoplasms. J Hematol Oncol 7: 96, 2014.
25. Favreau AJ and Sathyanarayana P: miR-590-5p, miR-219-5p, miR-15b and miR-628-5p are commonly regulated by IL-3, GM-CSF and G-CSF in acute myeloid leukemia. Leuk Res 36: 334-341, 2012.
26. Wu X, Zheng Y, Han B and Dong X: Long noncoding RNA BLACAT1 modulates ABCB1 to promote oxaliplatin resistance of gastric cancer via sponging miR-361. Biomed Pharmacother 99: 832-838, 2018.
27. Zhang S, Liu Z, Wu L and Wang Y: MiR-361 targets Yes-associated protein (YAP) mRNA to suppress cell proliferation in lung cancer. Biochem Biophys Res Commun 492: 468-473, 2017.
28. Chiyomaru T, Seki N, Inoguchi S, Ishihara T, Mataki H, Matsushita R, Goto Y, Nishikawa R, Tatarano S, Itesako T, *et al*: Dual regulation of receptor tyrosine kinase genes EGFR and c-Met by the tumor-suppressive microRNA-23b/27b cluster in bladder cancer. Int J Oncol 46: 487-496, 2015.
29. Ning S, Xu H, Al-Shyoukh I, Feng J and Sun R: An application of a Hill-based response surface model for a drug combination experiment on lung cancer. Stat Med 33: 4227-4236, 2014.
30. Xiao Q, Wang L and Xu H: Application of kriging models for a drug combination experiment on lung cancer. Stat Med 38: 236-246, 2019.
31. Li C, Li L, Zhou HH, Xia C and He L: Improving Yield of 1,3-diglyceride by whole-cell lipase fromA. NigerGZUF36 catalyzed glycerolysis via medium optimization. J Braz Chem Soc 26: 247-254, 2015.
32. Fang HB, Ross DD, Sausville E and Tan M: Experimental design and interaction analysis of combination studies of drugs with log-linear dose responses. Stat Med 27: 3071-3083, 2008.
33. Zhang Y, Shi B, Chen J, Hu L and Zhao C: MiR-338-3p targets pyruvate kinase M2 and affects cell proliferation and metabolism of ovarian cancer. Am J Transl Res 8: 3266-3273, 2016.
34. Mezlini AM, Wang B, Deshwar A, Morris Q and Goldenberg A: Identifying cancer specific functionally relevant miRNAs from gene expression and miRNA-to-gene networks using regularized regression. PLoS One 8: e73168, 2013.
35. Rosenthal AS, Dexheimer TS, Nguyen G, Gileadi O, Vindigni A, Simeonov A, Jadhav A, Hickson I and Maloney DJ: Discovery of ML216, a small molecule inhibitor of bloom (BLM) helicase. Probe Reports from the NIH Molecular Libraries Program, Bethesda (MD), 2010.
36. Gupta A, Ahmad A, Singh H, Kaur S, K M N, Ansari MM, Jayamurugan G and Khan R: Nanocarrier composed of magnetite core coated with three polymeric shells mediates LCS-1 delivery for synthetic lethal therapy of BLM-defective colorectal cancer cells. Biomacromolecules 19: 803-815, 2018.

This work is licensed under a Creative Commons Attribution-NonCommercial-NoDerivatives 4.0 International (CC BY-NC-ND 4.0) License.